

Research Article**Open Access**

Low Discrimination of Charged Silica Particles at T4 Phage Surfaces

Madiha F. Khan¹, Hanjiang Dong², Yang Chen² and Michael A. Brook^{1,2*}¹Department of Biomedical Engineering, McMaster University, Canada²Department of Chemistry and Chemical Biology, McMaster University, Canada**Abstract**

Bacteriophages have a variety of interesting properties that can be exploited in biological assays, including high binding specificity for the identification of bioactive molecules, and particularly, their capacity to propagate via bacterial lysis. However, the development of phage-based assays and disinfection devices is hampered by ineffective methods to stabilize and orient the phage in active form. For example, T4 phage, which has an anionic head and cationic tail, binds targets using its tail fibers, hence the adsorption of their tails to a substrate during immobilization, limits the ability of T4 to bind targets. Previously, we demonstrated that T4 phage retains infectivity despite adsorption to large silica particles of anionic or cationic charge. In an effort to better understand this phenomenon, we have instead used silica nanoparticles – much smaller than the phage – to probe the locus of preferential adsorption. Silica nanoparticles (NPs) (10 and 30 nm) were synthesized from tetraethoxysilane (TEOS) using the Stöber process. Charged particles were prepared by mixing appropriate silica dispersions with the cationic polyelectrolyte (PDADMAC), leading to both negative (zeta potential ($\zeta < -10$) and positively charged ($\zeta > +10$) silica surfaces. These particles were mixed with 1.5×10^{10} pfu/mL T4 (model) phage and analyzed by transmission electron microscopy (TEM). Results show that regardless of the particle concentration, both positively and negatively charged 30 nm particles bind effectively to both head and tail, with a slight preference for the head. No difference between NP associations to head or tail was seen with 10 nm particles, possibly because of their lower charge surface density and smaller size, which can accommodate small features on the phage surface better. The high hydrophilicity of silica facilitates maintenance of phage hydration and, likely, phage mobility, such that orientation is less important for bacterial binding in this system.

Keywords: T4 bacteriophage (λ); Charged silica nanoparticles; Adsorption to phage surfaces; Transmission electron microscopy (TEM)

Introduction

Bacteriophages (phages) are naturally occurring, obligate parasites about 25-200 nm in length that infect bacteria [1]. They reproduce via a lysogenic or lytic cycle, the latter of which is commonly associated with bacterial lysis (death) and the release of viral progeny [2]. In each case, the initial adsorption and binding of phage to target bacterial cells is multivalent, strong and highly specific [3], like antibodies but significantly cheaper since phage can be cultured with ease [4]. As a consequence of their ubiquitous nature and general biocompatibility with non-target cells, the use of phage as nanobiosensors and biosorbents to capture, detect and identify bacteria is an active area of research [5,6].

Many phage-based assays require the tethering of phage onto a suitable substrate. This can be achieved by covalent binding of phage to surfaces via genetic modification of the phage [3,7]. However, such a strategy can yield low bacterial-capture efficiency due to incorrect phage orientation (infective regions must face away from the substrate and freely bind targets), while modified phages exhibit lower burst sizes (average number of phage produced per infected bacterium) and less infectivity than their unmodified counterparts, and can be labor or cost-intensive to produce [3,8]. An alternative and simpler immobilization strategy involves physical adsorption [9-12] of the phage using electrostatic attractions between the phage and substrate.

Phage carry a net negative charge [13] and can therefore be modified with cationic entities to facilitate tethering. Lamboy et al. demonstrated that cationic polymers show charge-dependent 'wrapping' around the phage (the higher the charge, the more effective the wrapping [14]), and the same concept was used by the Mangin group for the adhesion of T4 phage on paper using the cationic polymer PDADMAC [15].

In the case of T4 phage, the capsid and tail (infective region) are anionic and cationic, respectively [16], even though the overall charge is

negative. This charge differential was recently exploited to adsorb phage onto silica particle substrates for a bacterial capture assay [17]. Large (with respect to T4 phage, ~ 200 nm) porous silica spheres (~500 nm, diglyceryl siloxane (DGS) precursor) were rendered cationic, neutral or anionic by surface modification with different concentrations of aminopropyltriethoxysilane (APTS), monotriethoxysilyl-poly(ethylene glycol) (PEG), or N-(trimethoxysilylpropyl)ethylenediamine triacetic acid (ED3A), respectively. Phage did not adsorb effectively to surfaces modified with neutral groups, and those that did exhibited reduced infectivity. By contrast, four different phage adsorbed strongly to charged silica surfaces, and active phage remained bound to silica particles even after 15 consecutive wash steps (centrifugation and resuspension), which suggest that immobilization via electrostatic attraction is a viable technique for phage-based assay development. Interestingly, and contrary to predictions based on the charge differential for T4, the retention of activity was seen not only for phage adsorbed to cationic particles, but also for those bound to anionic spheres.

Since silica is inexpensive, environmentally friendly, and easy to synthesize in a variety of motifs, it has potential use in biosensors based on yeast, bacteria and other biomolecules [18-22]. In the case of phage, it will be necessary to better articulate phage interactions with charged

***Corresponding author:** Brook MA, Department of Chemistry, McMaster University, 1280 Main St. W., Hamilton, Ontario, L8S 4M1, Canada, Tel: (905) 525-9140 23483; Fax: (905) 522-2509; E-mail: mabrook@mcmaster.ca

Received June 19, 2015; **Accepted** September 07, 2015; **Published** September 09, 2015

Citation: Khan MF, Dong H, Chen Y, Brook MA (2015) Low Discrimination of Charged Silica Particles at T4 Phage Surfaces. *Biosens J* 4: 125. doi:10.4172/2090-4967.1000125

Copyright: © 2015 Khan MF, et al. This is an open-access article distributed under the terms of the Creative Commons Attribution License, which permits unrestricted use, distribution, and reproduction in any medium, provided the original author and source are credited.

silica. To do so, an understanding of the effect of charges on a different scale is required. Previous work involved silica surfaces that were much larger than the phage and would present essentially flat surfaces (Figure 1A and 1B) [17]. Instead, therefore, we have decided to probe the silica phage interactions using charged silica particles that are much smaller than the phage. The particles were allowed to self-select phage domains to which they have best affinity.

Materials and Methods

Tetraethoxysilane (TEOS, 98%), methanol (MeOH), ammonium hydroxide (28%), and poly(diallyldimethylammonium chloride) (PDADMAC, 20% w/w, MW=100-200 K) were purchased from Sigma-Aldrich. Ethanol (EtOH) was obtained from Commercial Alcohols. All chemicals were used as received. All water was twice distilled and deionized to a specific resistance of at least 18 MΩ cm using a Milli-Q synthesis A10 water purification system. Purified T4 phages (1.5×10^{12} pfu/mL) were provided by the Griffiths lab at the University of Guelph.

Synthesis of silica NPs

Silica NPs were prepared by the well-known Stöber process (hydrolysis and condensation of TEOS in alcohol solvent in the presence of ammonium hydroxide) [23]. For the preparation of 10 nm particles, 30 mL MeOH, 1.6 mL H₂O, and 0.16 mL NH₄OH were mixed in a 250 mL flask, to which a mixture of 10 mL TEOS and 40 mL MeOH was quickly added. For the preparation of 30 nm particles, 35 mL EtOH and 3 mL NH₄OH were mixed in a 250 mL flask, to which a mixture of 6 mL TEOS and 40 mL EtOH was quickly added. All experiments were carried out at room temperature under magnetic stirring at a rate of 500 rpm for 24 h. For the 10 nm particles, 4 M HNO₃ was added after 24 h to bring the solution pH to 2.7, to ensure that the particles would remain stable in solution. The particles were then washed and re-suspended several times in DI water. The concentrations of 10 and 30 nm silica nanoparticles thus obtained were 80 and 20 mg/mL, respectively. The concentrations of 10 and 30 nm particles were adjusted to 0.8 mg/mL,

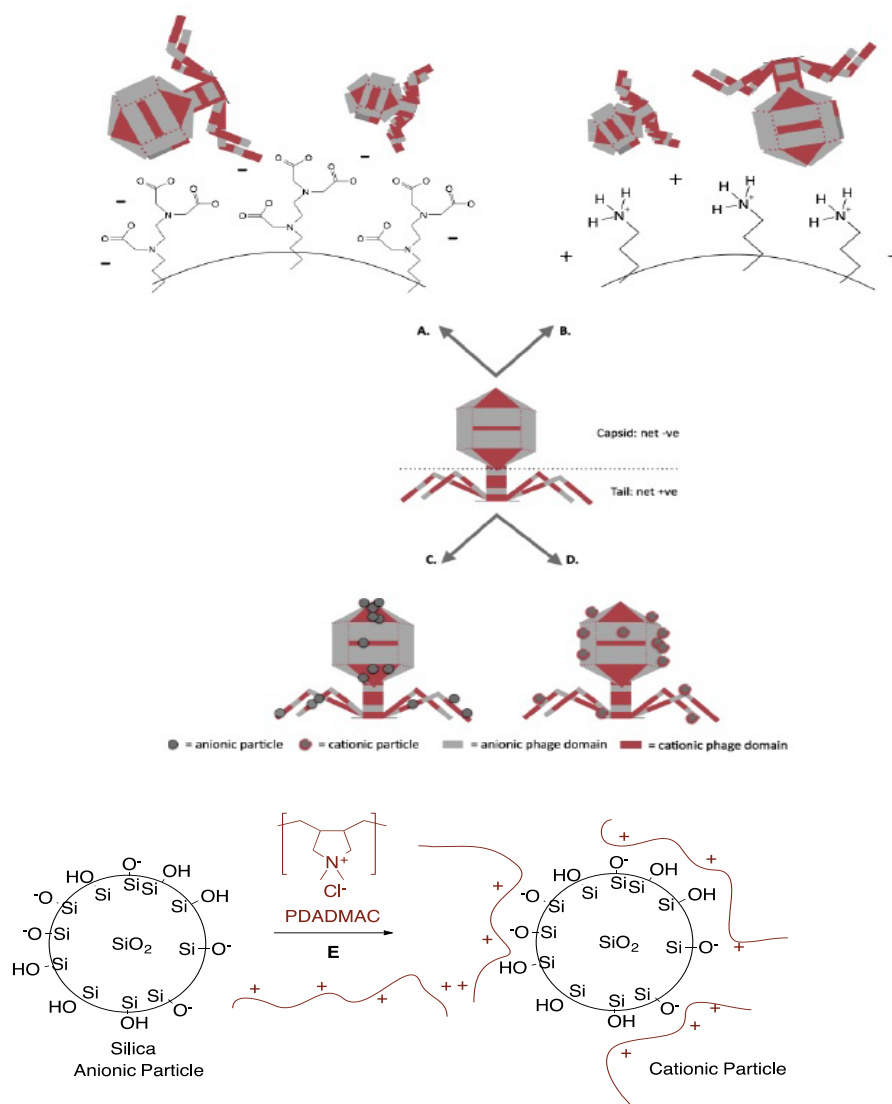


Figure 1: Model interaction of T4 (A) bacteriophage with large particles of A: anionic silica and B: cationic silica [17] and small particles of C: anionic silica and D: cationic silica prepared by E: adsorption of poly(diallyldimethylammonium chloride) PDADMAC to negatively charged silica particles.

0.16 mg/mL, and 0.032 mg/mL (10 nm) and 2 mg/mL, 0.8 mg/mL, and 0.4 mg/mL, respectively by appropriate dilutions.

Preparation of positively charged silica NPs

Positively charged silica particles were prepared by mixing 1 mL silica stock solution and 0.5-10 μ L polyelectrolyte solution (10% in deionized water) and then sonicating for 10 min. The electrophoretic mobility values of the resulting modified particles were measured by electrophoretic light scattering at 25 °C using a Brookhaven Zeta Potential Analyzer (Holtville, NY) with a 26 mW laser. Surface charge (zeta potential, ζ) of the particles was calculated from the mobility values thus obtained. In each case, 10 measurements were taken and the standard deviation used as an estimate of experimental variability. Excess PDADMAC was removed by the thrice-repeated process of centrifugation (15000 rpm, 30 min) followed by a water wash/redispersion (sonification 30 min) step (Figure 1E). Polymer coated 10 and 30 nm NPs were diluted to ensure they had the same concentrations as the unmodified anionic silica particles.

Preparation and imaging of silica-phage composites

Distilled H₂O (500 μ L) and 50 μ L of purified T4 phage (1.5×10^{10} pfu/mL) were first placed in a 2 mL vial, followed by 10 μ L of the desired silica NPs dispersion. The sample was stirred at room temperature. After a 1 h reaction/incubation time, 2 μ L of the sample was loaded onto Formvar-coated, 200-mesh Cu grids, allowed to sit for 2 min to ensure adsorption of phage onto the grids, and then stained with 2% (w/v) phosphotungstic acid dye (obtained from Sigma Aldrich) at pH 7.2. Any excess dye after 2 min was gently blotted using a KimWipe. The electron-dense phosphotungstic dye that adsorbs well to viruses served as a negative stain [24,25]. After air-drying for 10 min, the grids were viewed under a JEOL JEM 1200 EX TEMSCAN Transmission Electron Microscope (JEOL, Peabody, MA, USA) operating at an accelerating voltage of 100 kV. Three-six images were taken per sample from random points on the TEM grid using an AMT 4 megapixel digital camera (Advanced Microscopy Techniques, Woburn, MA). The entire preparation and imaging process was repeated for the different sizes, charges and concentrations of NPs, as well as the incubation times between phage and NPs (24 h, 1-2 weeks, Supporting information).

Quantification of T4-SiNP associations

The following criteria (Figure 2) were used to select images for quantification: (1) the image had clearly visible NPs in good contrast to the background; (2) the phage and the NPs in the image appeared as relatively discrete entities with minimal overlap (so as not to obscure particle counts); and (3) some (if not all) phages in the image had

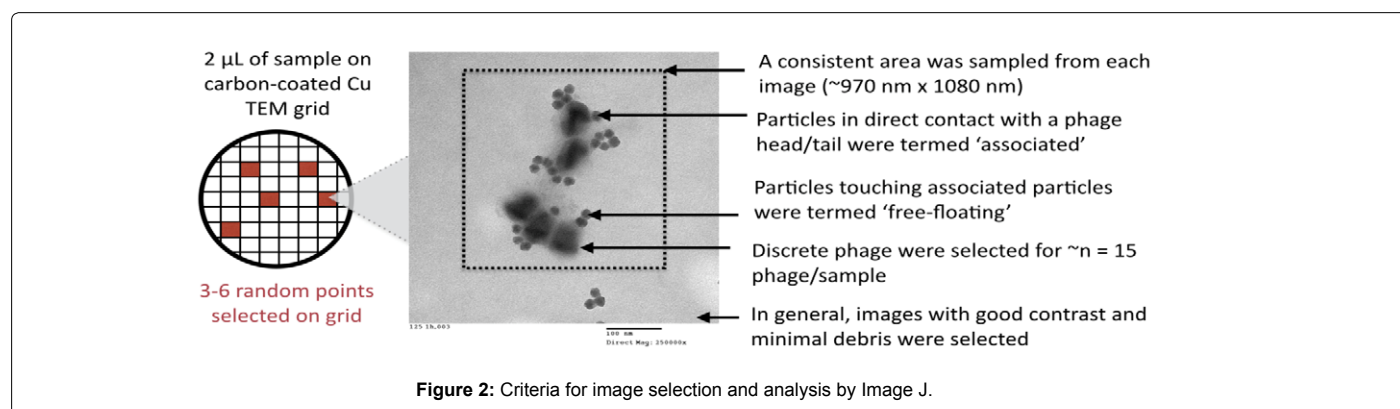
clearly visible heads and tails so that the NP associations between the head and tail on the same phage could be more accurately gauged. These data were used to select the optimal concentration of particles/phage, which occurred at lower concentrations. From each sample, care was taken to count particle associations with at least 15 phages, hence more than three images/sample were sometimes quantified. Since the magnifications of these images differed, care was also taken to ensure phages were counted from a consistent area across the images being analyzed (~ 970 nm \times 1080 nm). Particles in direct contact with a phage head or tail were counted as particles that were associated with the head/tail. Particles not touching the head/ tail but touching particles localized on the head were counted as 'free-floating' to try and minimize the effects of sample preparation for TEM (sample drying can cause structures to aggregate on the grid that were not associated in solution). All associated particles were counted manually, while the total number of particles in the image were counted using Image J. Counts by the latter required optimization so that there was good accordance between manual and software counts (see Supporting Information for a detailed procedure). The numbers of associated particles at each location on the phages (head/tail) were plotted. Statistical analysis was conducted using the two-sample t-test assuming unequal variances for the 10 nm particles (the preferences of cationic and anionic particles for phage head/tail were analyzed separately). Tests for statistical significance could not be conducted with 30 nm particles since the measurements from triplicate samples could not always be obtained.

Results

Differently sized (10 nm and 30 nm) native silica particles, which are negatively charged, were modified to different degrees by the addition of the positively charged polyelectrolyte, PDADMAC (Figure 1). After modification, the silica surfaces were either negatively charged (NC $\zeta < -10$) or positively charged (PC $\zeta > +10$), depending on the amount of PDADMAC added, as shown from zeta potential (ζ) values determined from particle electrophoretic mobility (μ E, Table 1). NP1 and NP4 (native, unmodified particles, negatively charged NC, 30 and 10 nm, respectively), and NP3 and NP6 (cationic particles PC, 30 and 10 nm, respectively) were used for subsequent experiments. Particles of different sizes were modified with the same amount of PDADMAC (500 μ L of silica NPs to 100 μ L of PDADMAC): NP3 exhibited a positive charge of 28.17 ± 1.44 , while NP6 carried a charge of 12.72 ± 0.38 due to the higher surface area.

Effect of concentration

Different concentrations of NP1 and NP3 particles, respectively, were mixed with 1.5×10^5 pfu/mL T4 phage prior to imaging. TEM



Nanoparticles	Diameter (nm)	Silica (μL)/ PDADMA (μL)	Zeta potential (ζ)	Mobility (μE)
NP1	30	500/0	-25.38 ± 2.95	-1.98 ± 0.23
NP3	30	500/100	28.17 ± 1.44	2.20 ± 0.11
NP4	10	500/0	-20.25 ± 2.25	-1.75 ± 0.27
NP6	10	500/100	12.72 ± 0.38	0.99 ± 0.03

Table 1: Zeta (ζ) potential of native, neutral and cationic silica nanoparticles).

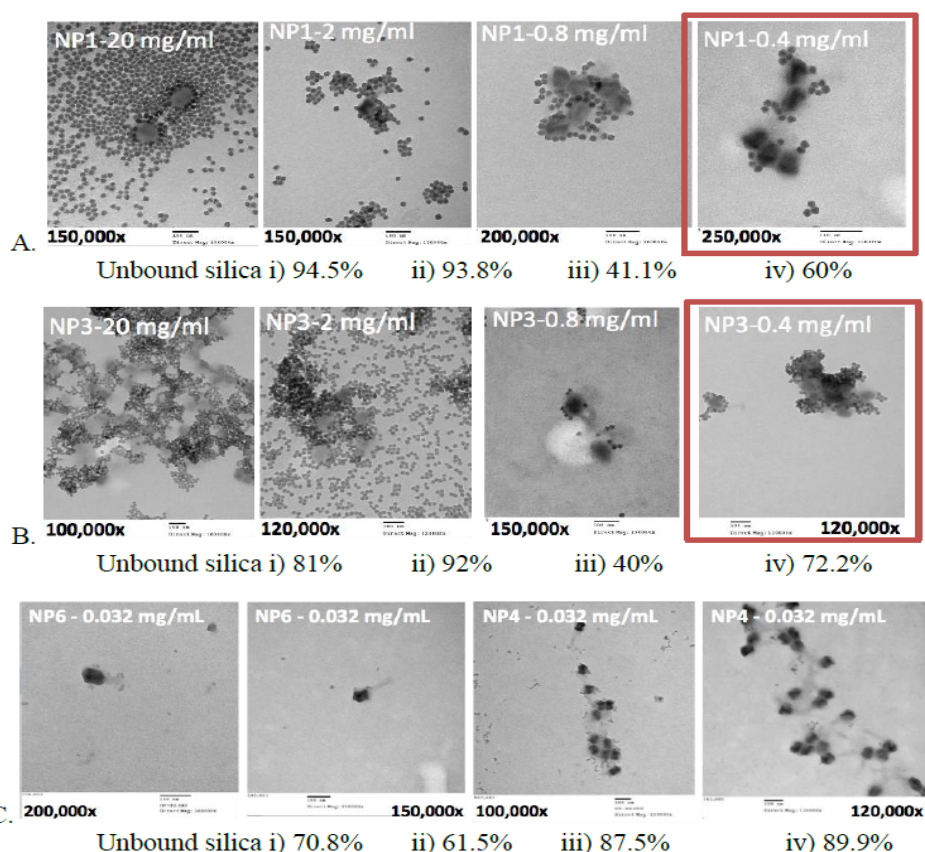


Figure 3: Select (and representative) TEM images for negatively and positively charged 30 nm particles A) NP1 and B) NP3 at 20, 2, 0.8 and 0.4 mg/mL each mixed with 1.5×10^{10} pfu/mL T4 phage. Both the 0.4 mg/ml negatively and positively charged particles show a preference for the negatively charged head. Unbound silica refers to the fraction of silica particles not associated with phage, compared to the total silica particle population. The TEM images in C) show the interactions between cationic (NP6) and anionic (NP4) 10 nm particles and phage (0.032 mg/mL).

images of the samples (Figure 3) showed that higher concentrations of particles (20 mg/mL and 2 mg/mL) formed gross aggregates of silica particles, and resulted in the complete and indiscriminate coating of phages, such that they were no longer clearly identifiable. Most silica particles were found in dense aggregates that did not contain phage (Figure 3Ai, Bi,ii, Ci, Supporting information).

In an attempt to examine particle and phage interactions more clearly, experiments and imaging for the other two variables, charge and size, were conducted only for particles at the lowest concentrations (0.4 mg/mL for 30 nm particles and 0.032 mg/mL for 10 nm particles, respectively). These lower concentrations allowed for better quantification of silica/phage association: in many cases the nanoparticles did not completely coat the phage surface allowing one to establish particle selectivity for the capsid or tail, as seen in Figure 3.

Effect of particle charge and charge density

NP1 and NP3 (0.4 mg/mL) were mixed with 1.5×10^5 pfu/mL T4 phage for 24 h or 1-2 weeks (Supporting information), respectively, prior to imaging and then quantification with Image J. The average number of silica NPs found at the head/ tail of the phages is plotted in Figure 4A and 4B. As is evident from the Figure, and contradictory to initial predictions, nanoparticle interactions with the phage were not limited to the areas of opposite charges; cationic particles were also found adsorbed to cationic tails and anionic particles were found on anionic capsids. Irrespective of the silica particle charge, 30 nm particles were on average twice more likely to be associated with capsids than tails. In all cases, the highest capsid-NP associations were already evident after 1 hour of incubation.

It proved challenging with TEM to locate 10 nm particles on phage unless the silica had undergone some degree of aggregation. As

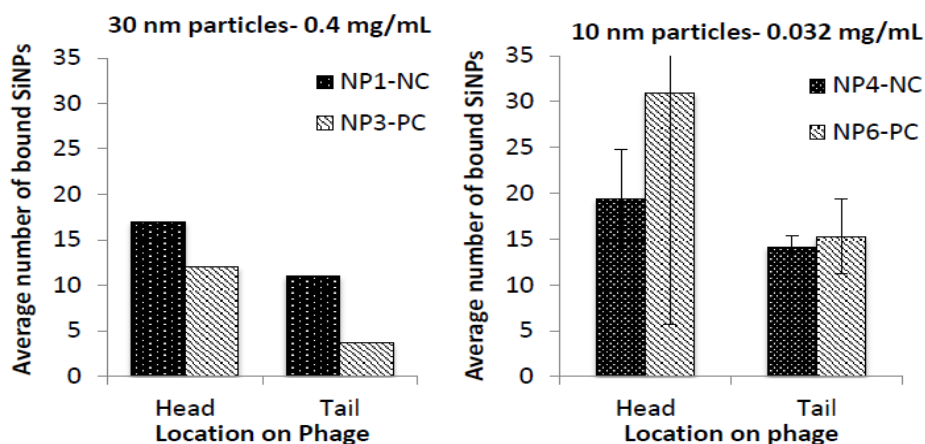


Figure 4: Particle binding after 24 hours on phages for A) negatively charged 30 nm particles (NP1-NC) and positively charged 30 nm particles (NP3-PC). B) Binding of negatively (NP4-NC) and positively (NP6-PC) charged 10 nm silica particles to phage.

a consequence, the numbers reported below (Figure 4) are likely to be an underrepresentation of the actual number of interactions that took place. The smaller nanoparticles showed even less discrimination than the 30 nm particles for adsorption with respect to phage location. The charge on silica was not important in this regard: negatively and positively charged particles were found in approximately equal numbers (with no statistically significant difference) at both the phage head and tail (two sample $t(1)=12.7$, $p=0.023$ for the difference in numbers between head and tail of cationic particles, and two sample $t(1)=12.7$, $p=0.35$ for the difference in numbers between head and tail of anionic particles). Note that the unit charge per surface area was lower than the 30 nm particles.

Discussion

The development of phage-based biosensors has gained much attention over recent years, owing to the need for simple and cost-effective detection of problematic bacteria in a variety of settings. Phages are highly specific in their binding to targets, generally inexpensive to culture in vitro, and relatively robust. However, many sensors based on phage exhibit poor bacterial capture efficiency due to incorrect phage orientation after immobilization on substrates. T4 phage, for example, must generally be immobilized head-down to leave the infective tails free for binding.

Previously, we demonstrated that charge could be utilized to anchor T4 phage onto silica particles that were much larger than the virus [17]. Both heads and tails of the negatively charge phages adsorbed to either anionic or cationic silica respectively (Figure 1A and 1B), and remained infective. We reasoned that the binding of small silica particles to phage, rather than phage to large silica surfaces, would provide a better understanding of the electrostatic demands of phage binding to silica.

At high concentrations, silica-silica particle aggregation dominated the colloidal behavior of phage samples with both types of silica particles. The situation was caused, in part, by the drying of the dispersion on the TEM grid (Figure 3). Samples were air-dried prior to imaging, and in the evaporating droplet, the concentration of nanoparticles likely increased until van der Waals attractions overcame

repulsive forces causing increased particle collision and aggregation. Two additional factors could have exacerbated this phenomenon: hydrophobicity of the TEM grid surface [26], and the different evaporation rates experienced by different areas of the droplet [27]. In the first case, the hydrophobicity of the formvar film would have forced the droplet to maintain a constant contact angle with the surface, thus minimizing the droplet's exposure to the grid. As a consequence, as the liquid evaporated the suspended colloids likely converged into an increasingly smaller area on the film. Silica aggregation was therefore facilitated as the particle concentration increased. This would also explain why the phage and SiNPs were not homogeneously distributed across the TEM grid. In the second case, differential evaporation of the droplet would have induced capillary flow from the center of the drop to its edges, resulting in net flow of particles outwards where they were deposited and substantially aggregated (Figure 3Ai and Bi).

When lower concentrations of silica particles were exposed to phage, as seen in Figure 3 and Figure 4, both 10 nm and 30 nm silica particles adsorbed efficiently across the entire phage surface. This results from the particles losing their colloidal stability, which in turn is facilitated by the loss of electrostatic stabilization that particles experienced upon their contact with the charged virus. It is important to note that the overall negative charge of the phage, and the positive and negative charges reported for the phage tail and head respectively, are net charges; they are a summation of the positive and negatively charged domains distributed across the virus, which is in effect, a complex polyelectrolyte. Evidence for this is the technique of phage display, which exploits the groups present at the external surface of phage to identify biomolecules with desired properties [28]. Hence, the effect of localized charges may account for the binding differences between 30 nm, 10 nm particles and the phages seen herein.

The 30 nm cationic particles, for example, appeared to prefer the head in comparison with the anionic particles, but only by less than a factor of ~ 2 . By contrast, the anionic particles seemed to bind as well to the head as they do to the tail. The larger (30 nm) particles had a slightly higher cationic charge than the 10 nm particles (Table 1) because of a higher PDADMAC loading per surface area (NP6 v NP3; 12.72 ± 0.38 v 28.17 ± 1.44), which may have caused the higher selectivity for anionic

surface residues on the phage. The ability of the 10 nm particles to adsorb effectively across the entire phage surface may also be affiliated with a greater ease of adapting to local domains because of their smaller size.

Based on these results, our initially naïve view can be refined: gross net charge (which causes cationic polymers to wrap around the phage [14]) do not predominate electrostatic interactions with small silica particles. Furthermore, since phage adsorb to large cationic and anionic silica surfaces without preference (Figure 1A and 1B) [17], the size of the phage-binding particle is clearly important. It may be that regions of small charged peptides bind strongly to charged silica nanoparticles of comparable sizes, and the higher the charge on the peptide, the higher the binding affinity [29].

One of the main advantages of electrostatic binding of phage to large silica particles, was the maintenance of infectivity irrespective of the type of charge on the silica surface: if tails adsorbed preferentially to anionic particles, the phage was clearly able to realign to interact with bacteria. This implies high levels of hydration which, given silica's high surface energy and high hydrophilicity, is not surprising. The water can provide a mobile layer on which phage can move. The small particle data shown here further suggests strategies for stabilizing phage in hydrophilic domains by interaction with small negatively and/or positively charged silica particles: the electrostatic interactions may extend the longevity of phage in bioassays and without limiting binding of the tails. That is, binding of the silica, which stabilizes the phage, can be readily overcome by the presence of a bacterium. Attempting to exploit these interactions will be the basis of future reports.

Conclusions

Although T4 phage have a negatively charged capsid and positively charged binding tail, small silica particles effectively bind to both parts of the phage. Local charge domains are accessible to the 10 and 30 nm particles. The ability of phage to remain infective on silica supports may arise not only from the hydration provided by the electrostatically rich environment, and the 'balanced binding' which helps stabilize the phage, but which can be displaced by a bacterium to initiate the infection event.

Acknowledgments

We acknowledge with gratitude the financial support of Sentinel: NSERC Network on Bioactive Paper.

References

- Marks T, Sharp R (2000) Bacteriophages and biotechnology: A review. *Journal of Chemical Technology and Biotechnology* 75: 6-17.
- Echols H (1972) Developmental pathways for the temperate phage: Lysis vs lysogeny. *Annu Rev Genet* 6: 157-190.
- Tolba M, Minikh O, Brovko L, Evoy S, Griffiths M (2010) Oriented immobilization of bacteriophages for biosensor applications. *Appl Environ Microbiol* 76: 528-535.
- Vincent J, Mark L, Michel H, Hauke S, John VDO (2011) Alternative affinity tools: More attractive than antibodies?. *Biochem J* 436: 1-13.
- Sabour PM, Griffiths MW (2010) Bacteriophages in the control of food-and waterborne pathogens. American Society for Microbiology Press, Washington.
- Zourob M, Ripp S (2010) Bacteriophage-based biosensors. In: Zourob M (eds) *Recognition receptors in biosensors*, Springer.
- Sun W, Brovko L, Griffiths M (2001) Use of bioluminescent salmonella for assessing the efficiency of constructed phage-based biosorbent. *J Ind Microbiol Biotechnol* 27: 126-128.
- Minikh O, Tolba M, Brovko L, Griffiths M (2010) Bacteriophage-based biosorbents coupled with bioluminescent atp assay for rapid concentration and detection of escherichia coli. *J Microbiol Methods* 82: 177-183.
- Balasubramanian S, Sorokulova IB, Vodyanov VJ, Simonian AL (2007) Lytic phage as a specific and selective probe for detection of staphylococcus aureus-a surface plasmon resonance spectroscopic study. *Biosens Bioelectron* 22: 948-955.
- Bennett A, Davids F, Vlahodimou S, Banks J, Betts R (1997) The use of bacteriophage-based systems for the separation and concentration of salmonella. *J Appl Microbiol* 83: 259-265.
- Handa H, Gurczynski S, Jackson MP, Auner G, Walker J, et al. (2008) Recognition of salmonella typhimurium by immobilized phage p22 monolayers. *Surf Sci* 602: 1392-1400.
- Nanduri V, Bhunia AK, Tu SI, Paoli GC, Brewster JD (2007) Spr biosensor for the detection of I. Monocytogenes using phage-displayed antibody. *Biosens Bioelectron* 23: 248-252.
- Archer MJ, Liu JL (2009) Bacteriophage t4 nanoparticles as materials in sensor applications: Variables that influence their organization and assembly on surfaces. *Sensors* 9: 6298-6311.
- Lamboy JA, Arter JA, Knopp KA, Der D, Overstreet CM, et al. (2009) Phage wrapping with cationic polymers eliminates nonspecific binding between m13 phage and high p/target proteins. *J Am Chem Soc* 131: 16454-16460.
- Jabrane T, Dubé M, Mangin PJ (2009) Bacteriophage immobilization on paper surface: Effect of cationic pre-coat layer. *Proceedings of PAPTAC 95th Annual Meeting*, Quebec.
- Serwer P, Hayes SJ (1982) Agarose gel electrophoresis of bacteriophages and related particles. I. Avoidance of binding to the gel and recognizing of particles with packaged DNA. *Electrophoresis* 3: 76-80.
- Cademartiri R, Anany H, Gross I, Bhayani R, Griffiths M, et al. (2010) Immobilization of bacteriophages on modified silica particles. *Biomaterials* 31: 1904-1910.
- Besanger TR, Chen Y, Deisingh AK, Hodgson R, Jin W, et al. (2003) Screening of inhibitors using enzymes entrapped in sol-gel-derived materials. *Analytical chemistry* 75: 2382-2391.
- Brook MA, Chen Y, Guo K, Zhang Z, Jin W (2004) Proteins entrapped in silica monoliths prepared from glyceroxysilanes. *Journal of sol-gel science and technology* 31: 343-348.
- Sui X, Cruz-Aguado JA, Chen Y, Zhang Z, Brook MA (2005) Properties of human serum albumin entrapped in sol-gel-derived silica bearing covalently tethered sugars. *Chemistry of materials* 17: 1174-1182.
- Nassif N, Bouvet O, Rager MN, Roux C, Coradin T, et al. (2002) Living bacteria in silica gels. *Nature materials* 1: 42-44.
- Livage J, Coradin T, Roux C (2001) Encapsulation of biomolecules in silica gels. *Journal of Physics: Condensed Matter* 13: R673.
- Stöber W, Fink A, Bohn E (1968) Controlled Growth of Monodisperse Silica Spheres in the Micron Size Range. *J Colloid Interface Sci* 26: 62-69.
- Ackermann HW, DuBow MS (1987) *Viruses of prokaryotes: General properties of bacteriophages*. CRC Press, Michigan.
- Hayat MA, Miller SE (1990) *Negative staining*. McGraw-Hill Publishing Company, Michigan.
- Picknett RG, Bexon R (1977) The evaporation of sessile or pendant drops in still air. *Journal of Colloid and Interface Science* 61: 336-350.
- Deegan RD, Bakajin O, Dupont TF, Huber G, Nagel SR, et al. (1997) Capillary flow as the cause of ring stains from dried liquid drops. *Nature* 389: 827-829.
- Omidfar K, Daneshpour M (2015) Advances in phage display technology for drug discovery. *Expert Opinion on Drug Discovery* 10: 651-669.
- Patwardhan SV, Emami FS, Berry RJ, Jones SE, Naik RR, et al. (2012) Chemistry of aqueous silica nanoparticle surfaces and the mechanism of selective peptide adsorption. *J Am Chem Soc* 134: 6244-6256.